ELSEVIER

Journal of Organometallic Chemistry 524 (1996) 169–179

Journal of Organo metallic Chemistry

Organometallic-substituted allenes – determination of coupling signs and molecular structures of two stannylated allenes

Bernd Wrackmeyer *, Udo Dörfler, Gerald Kehr, Heidi E. Maisel, Wolfgang Milius

Laboratorium für Anorganische Chemie, Universität Bayreuth, D-95440 Bayreuth, Germany

Received 8 March 1996; in revised form 23 April 1996

Abstract

The stannylated allenes **1** and **2** were prepared by 1,1-organoboration of two equivalents of bis(trimethylstannyl)ethyne (**4**) with one equivalent of triethylborane or ferrocenyl–dimethylborane. The organometallic-substituted alkenes **5** and **6** could be obtained from 1 : 1 reactions. 4-(9-Borabicyclo[3.3.1]non-9-yl)-1,1,4,4-tetrakis(trimethylstannyl)-1,2-butadiene (**3**) was obtained from the reaction of **4** with dimeric 9-borabicyclo[3.3.1]nonane. The molecular structures of the allenes **1** and **3** were determined by X-ray analysis. In both cases, the structural parameters of the $(Me_3Sn)_2C-BR_2$ unit indicate Sn–C hyperconjugation, and this model is supported by the small magnitude of the coupling constants $^1J(^{119}Sn, ^{13}C)$, by the increased ^{11}B nuclear shielding as well as by the unusual changes in the $\delta^{119}Sn$ values in going from the solution to the solid state. A fairly complete set of signs of coupling constants $^nJ(^{119}Sn, ^1H)$, $^nJ(^{119}Sn, ^{13}C)$ and $^nJ(Sn, Sn)$ was derived for the allene **3** using 2D $^{13}C/^1H$ and $^{119}Sn/^1H$ heteronuclear shift correlations.

Keywords: Allenes; Organotin compounds; 1,1-Organoboration; Hyperconjugation; NMR; Boron; Crystal structure; Tin

1. Introduction

Allenes bearing stannyl groups or other organometallic substituents are attractive reagents in synthesis [1]. It was shown that 1,1-organoboration of certain alkynyltin compounds [2] provides a convenient route to allenes of type **A** [3–5]. A fairly complex reaction mechanism was discussed, and the proposed molecular structure of these allenes was based mainly on NMR spectroscopic evidence. Although an extensive data set had been collected [3–5], these data were not complete as far as some coupling constants [$J(^{119}Sn, ^{13}C)$ or $J(Sn, Sn)$] and their signs are concerned.

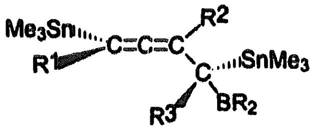

A

R = alkyl
R^1 = ^{t}Bu, $SiMe_3$, $SnMe_3$
R^2 = H, alkyl
R^3 = H, Me, $SiMe_3$, $SnMe_3$

We have now studied some of the compounds of type **A** again in order to improve the NMR data set, using modified 1D techniques for observing ^{13}C NMR signals of quaternary carbon atoms linked to boron, and applying 2D methods for the determination of absolute coupling signs. Furthermore, we have aimed to confirm the proposed molecular structure of allenes of type **A** by X-ray analyses. In this context, structural parameters of the group $C(SnMe_3)(R^3)BR_2$ were of particular interest, since hyperconjugative interactions (or σ–π delocalization as a general term) should be revealed by elongation of the Sn–C and shortening of the B–C bond lengths. Hyperconjugation should be significant owing to Me_3Sn groups in β-position with respect to the electron deficient trigonal planar boron atom [6].

2. Results and discussion

2.1. Synthesis

The allenes **1**–**3** were obtained from the reaction of triethylborane Et_3B, ferrocenyl–dimethylborane $Fc-BMe_2$, and dimeric 9-borabicyclo[3.3.1]nonane $(9-BBN)_2$ with bis(trimethylstannyl)ethyne (**4**) [Eqs. (1)–(3)], as described previously for **1** and **3** [3–5].

The organometallic-substituted alkenes **5** [7] and **6** were characterized as intermediates, whereas no intermediate could be detected when the reaction according

* Corresponding author.

0022-328X/96/$15.00
PII S0022-328X(96)06436-4

to Eq. (3) was monitored by [119]Sn NMR spectroscopy between −78 and 25°C. This is the second report on ferrocenylboranes taking part in the 1,1-organoboration of alkynyltin compounds [8]. It was found [8] that Fc–BMe_2 reacts with trimethyl-1-propynyltin, Me_3Sn–C≡CMe via 1,1-organoboration to give a mixture of alkenes resulting from transfer of either the methyl or the ferrocenyl group. In contrast, the reaction of Fc–BMe_2 with **4** affords selectively the alkene derivative **6** [identified by its NMR data (see Table 2)] by transfer of the methyl group from the boron to the alkynyl carbon atom. Compound **6** reacts with a second equivalent of bis(trimethylstannyl)ethyne (**4**) to give finally the allene **2**.

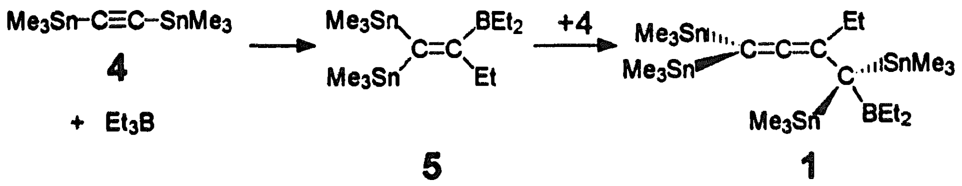

(1)

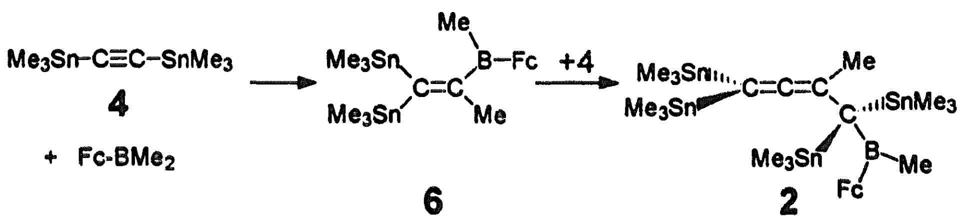

(2)

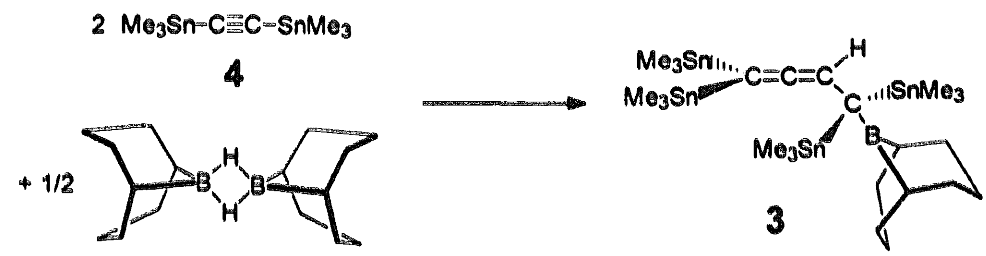

(3)

The allenes **1–3** are air- and moisture-sensitive, colourless (**1**, **3**) or red (**2**) solids which are readily soluble in benzene, toluene and chlorinated hydrocarbons. They can be purified by recrystallization from hexane or benzene. Under these conditions crystals suitable for X-ray analyses were obtained for **1** (from hexane) and **3** (from benzene).

For the formation of allenes of type **A**, including the allenes **1–3**, a mechanism is likely which requires first an intermediate **B** with a butadiene structure as a result of 1,1-organoboration starting from the organometallic-substituted alkenes of type **5** or **6** [Eq. (4a)]. Then, it is suggested that if R^1 is a bulky group (e.g. ^{t}Bu, $SiMe_3$, $SnMe_3$) **B** is converted to the allene structure by an irreversible allylic rearrangement [Eq. (4b)].

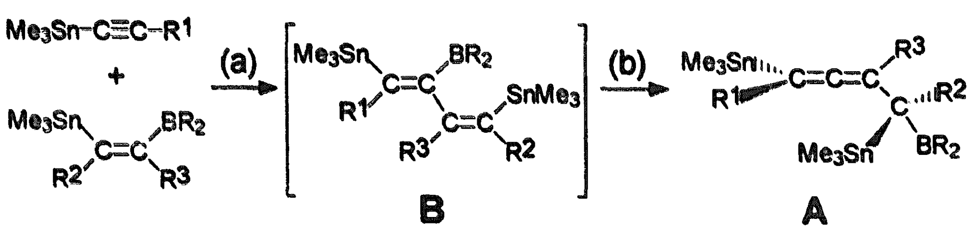

(4)

Table 1
Experimental data related to the single crystal X-ray analysis of the allenes **1** and **3**

	1	**3**
Formula (molecular mass)	$C_{22}H_{50}BSn_4$ (799.81)	$C_{24}H_{51}BSn_4$ (825.24)
Crystal; size (mm^3)	Colourless, isometric; 0.42 × 0.38 × 0.35	Colourless, prismatic; 0.30 × 0.30 × 0.60
Crystal system; space group; Z	Triclinic; $P\bar{1}$; 2	Monoclinic; $P2_1/n$; 4
Unit cell dimensions (pm); (°)	a = 968.0(2), b = 997.1(2), c = 1715.3(2); α = 106.29(2), β = 96.79(2), γ = 95.73(2)	a = 1461.5(2), b = 1265.7(2), c = 1800.2(2); β = 109.01(2)
V (pm^3 × 10^6)	1562.5(5)	3148.4(7)
Absorption coefficient (mm^{-1})	3.165	3.145
Diffractometer; radiation (pm)	Siemens P4; Mo Kα 71.073 (graphite monochromator)	
Temperature (K)	173	173
2θ-range	3.0 to 50.0°	4.0 to 50.0°
Scan type	ω	ω
Scan range (ω)	1.10°	1.20°
Measured reflections	6504	7066
Independent/observed reflections	5446 (R_{int} = 0.84%)/5446 ($F > 0.0\sigma(F)$)	5461 (R_{int} = 1.65%)/5461 ($F > 0.0\sigma(F)$)
Refined parameters	245	263
Solution	Direct methods (SHELXTL PLUS, VMS)	
Absorption correction	Empirical, Ψ scans	
T_{min}/T_{max}	0.2150/0.2686	0.0115/0.00421
Weighting scheme	$w^{-1} = \sigma^2(F) + 0.000F^2$	
R value/wR value (%) (refined against F)	2.08/1.64	2.71/1.98
Max./min. residual electron density (e pm^{-3} × 10^{-6})	0.74/−0.36	0.57/−0.42

2.2. X-ray structural analyses of the allenes 1 and 3

Experimental data relevant to the X-ray analyses of the allenes **1** and **3** are given in Table 1 [9]. The molecular structures of **1** and **3** are shown in Figs. 1 and 2 respectively, together with selected bond lengths and angles. In both cases, the structures proposed previously on the basis of spectroscopic data are confirmed, which also supports the suggested mechanism [3–5] (vide supra).

The two planes of the allene system form angles of 90° (**1**) and 84.7° (**3**), and there is only a small deviation from the expected linear arrangement of the allenic carbon atoms [bond angles C(1)–C(2)–C(3) 174.3(3)° (**1**) and 174.6(4)° (**3**)]. The C=C bond lengths are

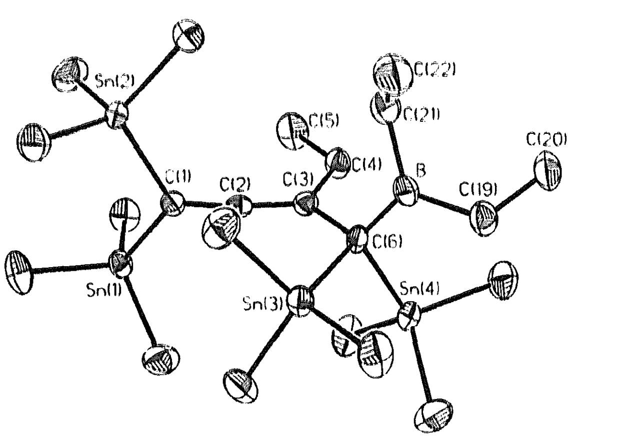

Fig. 1. Molecular structure of the allene **1**. Selected bond lengths (pm) and angles (°): Sn(1)–C(1) 215.7(3), Sn(2)–C(1) 215.8(3), Sn(3)–C(6) 222.1(3), Sn(4)–C(6) 219.5(3), C(1)–C(2) 129.7(4), C(2)–C(3) 131.9(4), C(3)–C(4) 152.5(4), C(3)–C(6) 152.5(4), B–C(6) 154.0(4), B–C(19) 159.0(5), B–C(21) 158.7(5); C(1)–C(2)–C(3) 174.3(3), Sn(3)–C(6)–B 99.5(2), Sn(4)–C(6)–B 114.4(2), C(6)–B–C(19) 122.9(3), C(6)–B–C(21) 120.8(3), C(19)–B–C(21) 116.3(3).

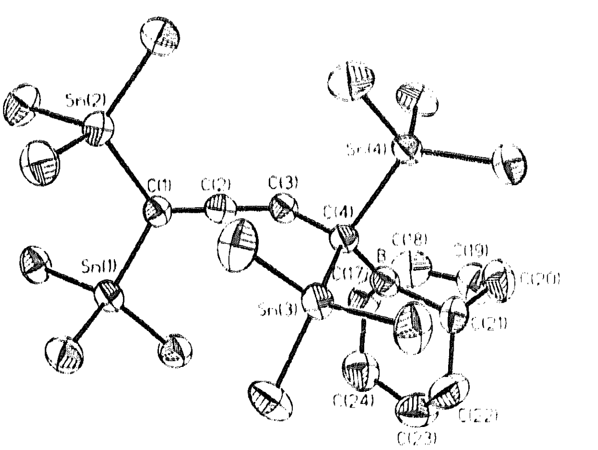

Fig. 2. Molecular structure of the allene **3**. Selected bond lengths (pm) and angles (°): Sn(1)–C(1) 215.0(4), Sn(2)–C(1) 216.1(4), C(1)–C(2) 129.3(5), C(2)–C(3) 131.4(5), C(3)–C(4) 152.8(5), B–C(4) 152.5(6), B–C(17) 158.6(6), B–C(21) 158.7(7); C(1)–C(2)–C(3) 174.6(4), Sn(3)–C(4)–B 107.9(2), Sn(4)–C(4)–B 108.1(2), C(4)–B–C(17) 125.0(4), C(4)–B–C(21) 126.3(3), C(17)–B–C(21) 108.8(4).

Table 2
^{11}B, ^{13}C and ^{119}Sn NMR data [a] of the organometallic-substituted alkenes **5** [b] and **6**

	5	6
$\delta^{13}C$		
$Sn_2C=$	138.0 [346.1, 298.0]	144.5 [290.9, 259.2]
$B-C=$	185.0	178.8
$=C-Et/Me$	36.9 [141.5, 118.2]	29.7 [141.0, 117.0]
	14.8 [9.1]	
$SnMe_3$	−5.3 [303.2, 10.4]	−5.5 [299.7, 9.9]
	−6.1 [310.4, 10.4]	−5.3 [312.9, 9.9]
BEt_2	21.6, 9.0	—
$B(Me)Fc$	—	8.5 (Me), 68.9 (Cp)
		75.1, 7.9 ($C^{2,5}$, $C^{3,4}$)
$\delta^{119}Sn$	−54.6 (*trans* to B)	−48.8
	−48.0 (*cis* to B)	−49.9
	[901] [c]	[913] [c]
$\delta^{11}B$	+84.0	+77.0

[a] Measured at 298 ± 1 K in toluene-d_8; coupling constants $^nJ(^{119}Sn, ^{13}C)$ and $^nJ(^{119}Sn, ^{117}Sn)$ in hertz are given in square brackets.
[b] Data taken from Ref. [7b]
[c] $^2J(^{119}Sn, ^{117}Sn)$.

slightly different, the shorter bond lengths being observed for C(1)–C(2) [129.7(4) pm (**1**), 129.3(5) pm (**3**)] and the longer ones for C(2)–C(3) [131.9(4) pm (**1**), 131.4(5) pm (**3**)]. In the allene systems, all bond lengths Sn–C and C–C as well as the bond angles are in the expected range.

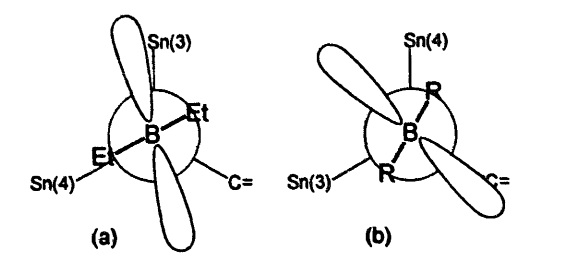

Fig. 3. Newman projections of the surroundings of (a) the B–C(6) and (b) the B–C(4) bonds showing the angles between the imaginary orientation of the unoccupied boron p_z orbital and the Sn–C(6) (**1**) and Sn–C(4) bonds (**3**) [(a) 12.5 and 61.6°; (b) 44.9 and 36.1°].

This is not the case for the surroundings of the carbon atom C(6) in **1** and C(4) in **3**, both bearing three organometallic substituents. The bond lengths C(6)–B and C(4)–B are rather short [154.0(4) pm (**1**), 152.5(6) pm (**3**)] when compared with other bond lengths B–C in **1** or **3** (158.7 to 158.9 pm). In the case of compound **3**, the bond length C(4)–B [152.5(6) pm] is in the range normally found for C–C bond lengths [e.g. in **3**: C(3)–C(4) 152.8(5) pm]. Furthermore, all bond lengths Sn–C(6) or Sn–C(4) are significantly elongated [219.5(3) and 222.1(3) pm in **1**; 219.2(3) and 220.2(3) pm in **3**] when compared with other bond lengths Sn–C in **1** and **3** (213 to 215 pm).

As shown in Fig. 3(a), there is only a small angle of 12.5° between the imaginary orientation of the empty boron p_z orbital and a plane involving B, Sn(3) and

Table 3
^{11}B, ^{13}C and ^{119}Sn NMR data [a] of the allenes **1**–**3**

	1	2	3
$\delta^{13}C$			
$Sn_2C=$	85.1 [294.2, 7.3]	81.1 [295.0, 8.4]	80.4 [−280.0(^1J), +8.3(^4J)]
$=C$	93.5 [74.5, 35.4]	86.6 [77.1, 23.4]	76.4 [−63.8(^3J), −21.8(^2J)]
$=C=$	208.0 [35.3, 39.5]	209.9 [35.3, 40.9]	207.8 [+36.0(^2J), −39.2(^3J)]
$Sn_2(B)C$	50.3 [153.0, 25.5]	47.5 [158.8, 25.6]	33.3 [−149.0(^1J), +22.7(^4J)]
$=C(SnMe_3)$	−6.9 [324.2]	−5.7 [321.9, 8.4]	−7.5 [333.5]
$C(SnMe_3)_2$	−4.0 [313.5]	−3.7 [312.9, 8.4]	−4.8 [314.6, 8.0]
$=CR$	31.2 [34.7, 25.6]	27.5 [34.2, 28.6]	—
	13.1		
BR	17.9, 9.3	13.1 [12.0]	29.5 (BC); 33.9 ($BCCH_2$);
		68.7 (Cp), 76.7 (C^1)	23.8 ($-CH_2-$) [b]
		75.0 ($C^{2,5}$), 72.1 ($C^{3,4}$)	
$\delta^{119}Sn$			
$=CSn_2$	−11.5 [424.0] [c]	−8.9 [415.0] [c]	−9.6 [+335.7] [c]
	[192.4, 187.5] [d]	[211.0] [d]	[+243.9, +233.4] [d]
CSn_2	−3.3 [440.0] [e]	+3.1 (broad)	+9.0 [−477.7] [e]
	[192.4, 187.5] [d]		[+243.9, +233.4] [d]
$\delta^{11}B$	+76.4	+68.0	+78.2

[a] Measured at 298 ± 1 K in toluene-d_8 if not mentioned otherwise; coupling constants $^nJ(^{119}Sn, ^{13}C)$ and $^nJ(^{119}Sn, ^{117}Sn)$ in hertz are given in square brackets.
[b] At 223 K in CD_2Cl_2: 30.1, 27.6 (BC); 34.2, 32.8 ($BCCH_2$); 26.8, 23.7 ($-CH_2-$).
[c] $^2J(^{119}Sn, ^{117}Sn)$ across the allenic carbon atom.
[d] $^5J(^{119}Sn, ^{117}Sn)$.
[e] $^2J(^{119}Sn, ^{117}Sn)$ across the aliphatic carbon atom.

C(6) in **1**, a favourable situation for σ–π delocalization (the corresponding angle with the B, Sn(4), C(6) plane is 61.6°). This is also indicated by another unusual feature, the rather small bond angle Sn(3)–C(6)–B [99.5(2)°]. Furthermore, the distance Sn(3)–C(6) of 222.1(3) pm is significantly longer than all other Sn–C bonds in both **1** and **3**. In the case of **3**, a similar preference of σ–π delocalization arising from one of the Sn–C(4) bonds is not possible because of the steric requirements of the 9-BBN group; the angles between the imiginary orientation of the boron p_z orbital and the planes B, Sn(3), C(4) and B, Sn(4), C(4) are 44.9° and 36.1° respectively (Fig. 3(b)), and the bond angles at C(4) do not deviate much from the tetrahedral angle.

In summary, the structural features of the $(Me_3Sn)_2CBR_2$ unit in **1** and **3** are in support of Sn–C hyperconjugation, compensating to some extent for the electron deficiency of the boron atom [6], and corroborating the interpretation of chemical shifts $\delta^{11}B$ and coupling constants $^{1}J(^{119}Sn, ^{13}C)$ (vide infra). Hyperconjugation plays an important role in the stabilization of carbocations [10,11], the isoelectronic counterparts of trigonal boranes.

2.3. NMR spectroscopic results

The NMR data (^{11}B, ^{13}C, ^{119}Sn) of the new alkene derivative **6** are given in Table 2, together with the data of **5** for comparison; Table 3 lists NMR data (^{11}B, ^{13}C, ^{119}Sn) of the allenes **1–3**. Most data of **1** and **3** are in agreement with the literature [3–5].

We have measured some values $^{1}J(^{119}Sn, ^{13}C)$ in the allenes **1–3** for the first time. The broadened ^{13}C NMR signals of the quaternary aliphatic carbon atoms linked to boron and to two tin atoms become sharp at lower temperature owing to quadrupolar decoupling [12]. If there is no overlap with other signals, the $^{117/119}Sn$ satellites can be detected straightforwardly. In the case of **3**, there is overlap with ^{13}C NMR signals of the 9-BBN group. Suppression of these signals by an appropriate *J*-modulated NMR experiment [13] is readily achieved, and the coupling constant can be measured.

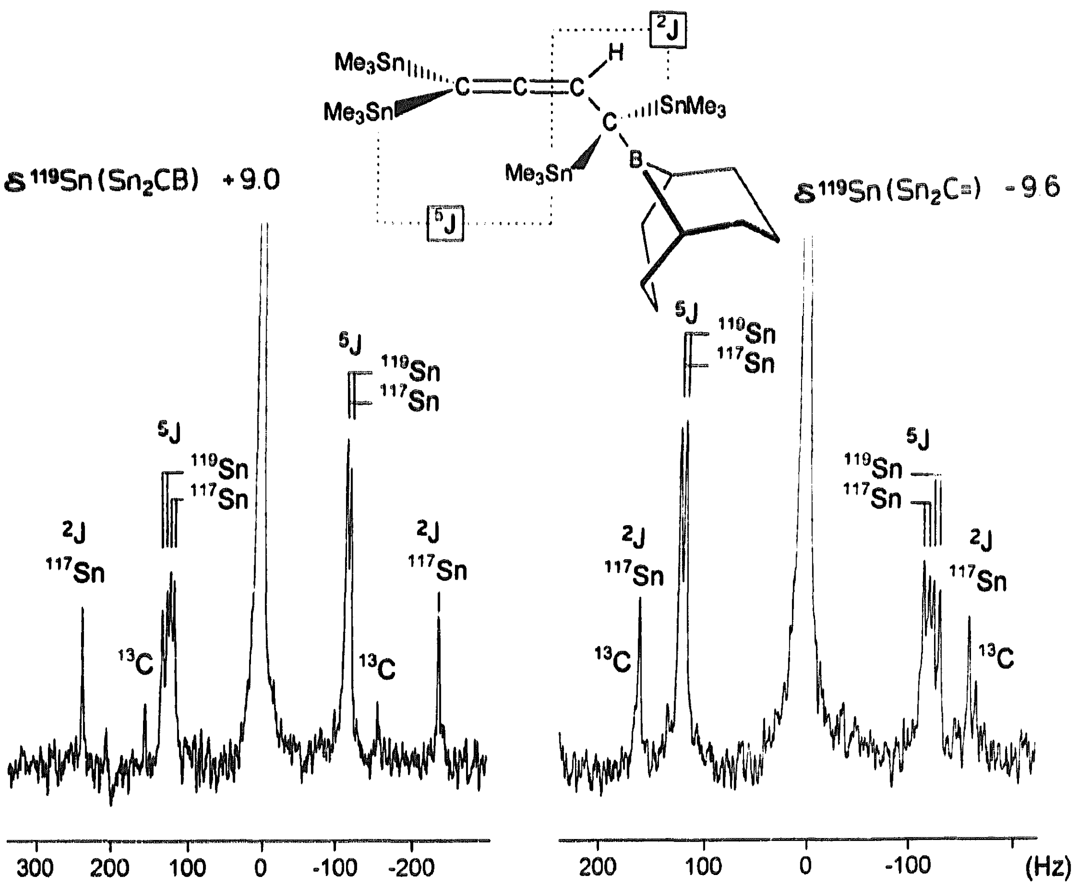

Fig. 4. 186.5 MHz ^{119}Sn NMR spectra of the allene **3** (recorded by using the refocused INEPT pulse sequence with ^{1}H decoupling [25]), showing the $^{117/119}Sn$ and part of the ^{13}C satellites. Note that there are two types of $^{5}J(Sn,Sn)$, since this particular isotopomer possesses two chiral centres and is therefore present as a pair of diastereomers.

The magnitude of these $|^1J(^{119}Sn, ^{13}C)|$ values is rather small when compared with the other data in Table 3 or in Ref. [4b]. This observation fits into the picture of Sn–C hyperconjugation owing to the neighbourhood of the electron deficient boron atom, as indicated by the elongation of the Sn–C(6) (**1**) and Sn–C(4) (**3**) bonds (vide supra). Small values $|^1J(^{119}Sn, ^{13}C)|$ are also typical of Me_3Sn-substituted methylene boranes [6], indicating Sn–C hyperconjugation in a similar way as small values $^1J(^{13}C, ^1H)$ found for H-bridged carbocations [14].

The J(Sn,Sn) values are fully assigned now in the case of **3** (Fig. 4). In the case of the allene **2**, the high frequency ^{119}Sn NMR signal (assigned to the $Sn_2(B)C$ group) is broad at room temperature as a result of hindered intramolecular rotation. This prevents the complete assignment of all J(Sn,Sn) values in **2**. ^{13}C and ^{119}Sn NMR measurements of **1–3** at low temperature show that the rotation about the $B–CSn_2$ and/or $Sn_2BC–C=$ bond becomes slow. However, it was not possible to distinguish four different ^{119}Sn NMR signals in solution, whereas the solid-state ^{119}Sn CP/MAS NMR spectrum of **1** reveals the expected four different sites (see Fig. 5). Unfortunately, most of the information on J(Sn,Sn) in the solid state is lost owing to the poorly resolved broad satellites. There are fairly large differences between $\delta^{119}Sn$ values of **1** in solution and in the solid state, and the solution-state $\delta^{119}Sn$ values do not correspond to the average of the solid-state $\delta^{119}Sn$ values. This can be explained by Sn–C hyperconjugation which is dependent on the orientation of the C_2B plane of the boryl group with respect to the Sn–C bonds. The $\delta^{11}B$ values of **1** (δ 76.4), **2** (δ 68.0) and **3** (78.2) are shifted by 9–10 ppm to lower frequencies when compared with trialkyl- or dialkylferrocenylboranes [15]. This increase in ^{11}B nuclear shielding is interpreted as the result of Sn–C hyperconjugation.

We have carried out sign determinations of coupling constants. The compound **3** was the best candidate for this purpose because scalar coupling between the allenic proton and ^{13}C or $^{117/119}Sn$ nuclei provides an excellent base for 2D heteronuclear shift correlations (HETCOR). If there are spin systems containing a pair of active spins (A,M) and one passive spin (X), the HETCOR experiments enable one to compare signs of coupling constants J(A,X) and J(M,X). A positive tilt in the contour plots for relevant cross peaks indicates alike signs, a negative tilt indicates different signs [16]. It is advisable to use the concept of reduced coupling constants K $[K(A, X) = 4\pi^2 J(A, X)(\gamma_A \gamma_B h)^{-1}]$ if nuclei are involved for which the gyromagnetic ratio is less than 0 (e.g. in the case of ^{119}Sn or ^{117}Sn). If the absolute

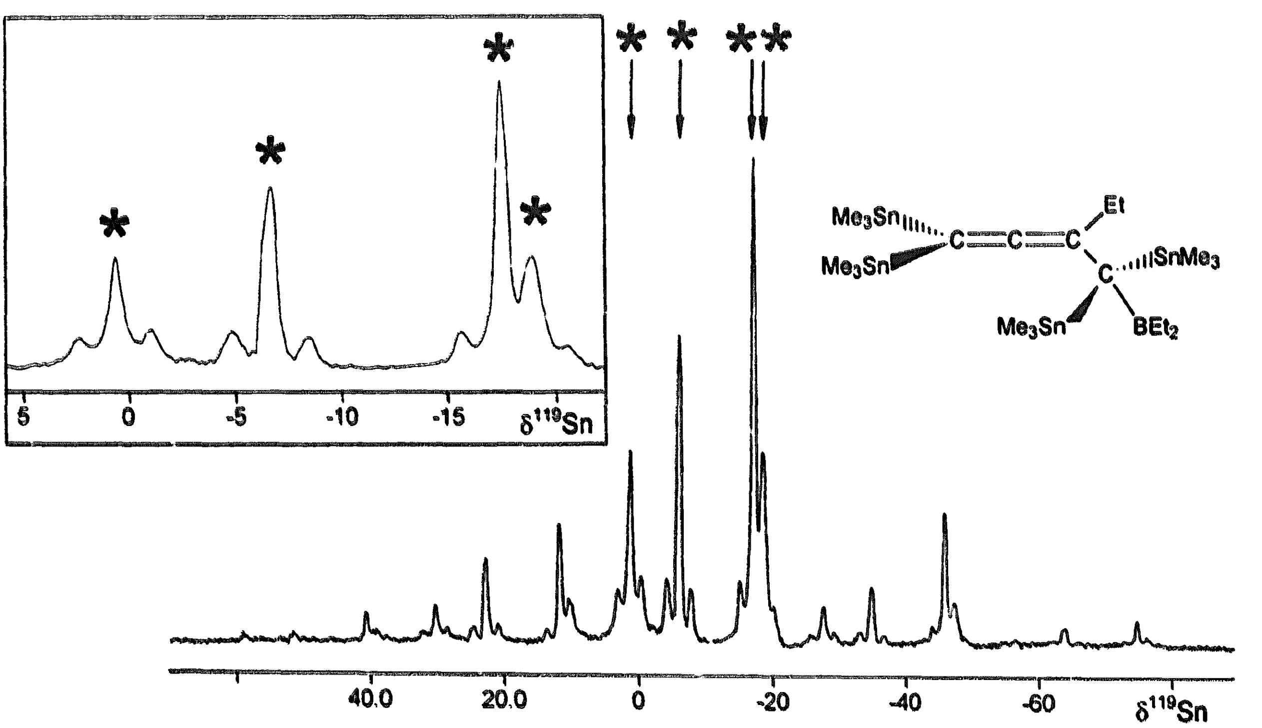

Fig. 5. 111.9 MHz solid-state ^{119}Sn CP/MAS NMR spectrum of the allene **1** (contact time 1 ms; 90° pulses for ^1H and ^{119}Sn: 5 μs; repetition time 5 s; spinning sidebands 3254 Hz; sweep width 38500 Hz; digital resolution 9.4 Hz/pt; 14300 transients). The inset shows the expansion of the centre bands (marked by asterisks and arrows). The $^{117/119}Sn$ satellites are partly visible (corresponding to J(Sn,Sn) of around 395 to 410 Hz) but remain unresolved and cannot be properly assigned. Note the differences in nuclear shielding: $\delta^{119}Sn$(solution, 298 K) = −3.3 for $Sn_2(B)C$ and −11.5 for $Sn_2C=$; $\delta^{119}Sn$(solid state) = 1.0, −6.5, −17.4, −18.9.

sign of one of the coupling constants is known (e.g. ${}^2K({}^{119}Sn, {}^1H_{SnMe}) < 0$ [17]), information on the absolute signs of other coupling constants can be gained. So far, only a few stannylated allenes have been studied by these techniques [18,19].

In the case of the allene **3**, there are mainly four meaningful 2D ${}^{13}C/{}^1H$ HETCOR experiments (${}^{13}C$ and ${}^1H$ are the active spins and ${}^{119}Sn$ is the passive spin). Polarization transfer from ${}^1H(SnMe_3)$ to ${}^{13}C(=CSn_2)$ [based on ${}^3J(={}^{13}CSnC{}^1H)$] proves that the signs of ${}^2K({}^{119}Sn, {}^1H_{(SnMe)})$ and ${}^1K({}^{119}Sn, {}^{13}C=)$ are opposite: since it is known that ${}^2K({}^{119}Sn, {}^1H_{(SnMe)}) < 0$ [17], ${}^1K({}^{119}Sn, {}^{13}C=)$ must be positive. The next experiments use polarization transfer from the allenic proton (=C–${}^1H$) to the three ${}^{13}C$ nuclei of the allene system [based on ${}^1J(={}^{13}C, {}^1H)$, ${}^2J(={}^{13}C=C{}^1H)$ and ${}^3J({}^{13}C=C=C{}^1H)$ as shown in Figs. 6, 7 and 8.

The final information on coupling signs in **3** stems from ${}^{119}Sn/{}^1H$ HETCOR experiments in which ${}^{117}Sn$ functions as the passive spin. Results are shown in Fig. 9, proving that ${}^5J(Sn,Sn) > 0$ and that the geminal coupling constant across the aliphatic carbon atom ${}^2J(Sn,Sn) < 0$, whereas ${}^2J(Sn,Sn)$ across the allenic carbon atom has a positive sign. These experimentally determined signs of the geminal coupling constants ${}^2J(Sn,Sn)$ are in complete agreement with the signs predicted by the correlation between ${}^2J({}^{119}Sn, {}^{13}C)$ and ${}^2J(Sn,Sn)$ for comparable organotin compounds [20].

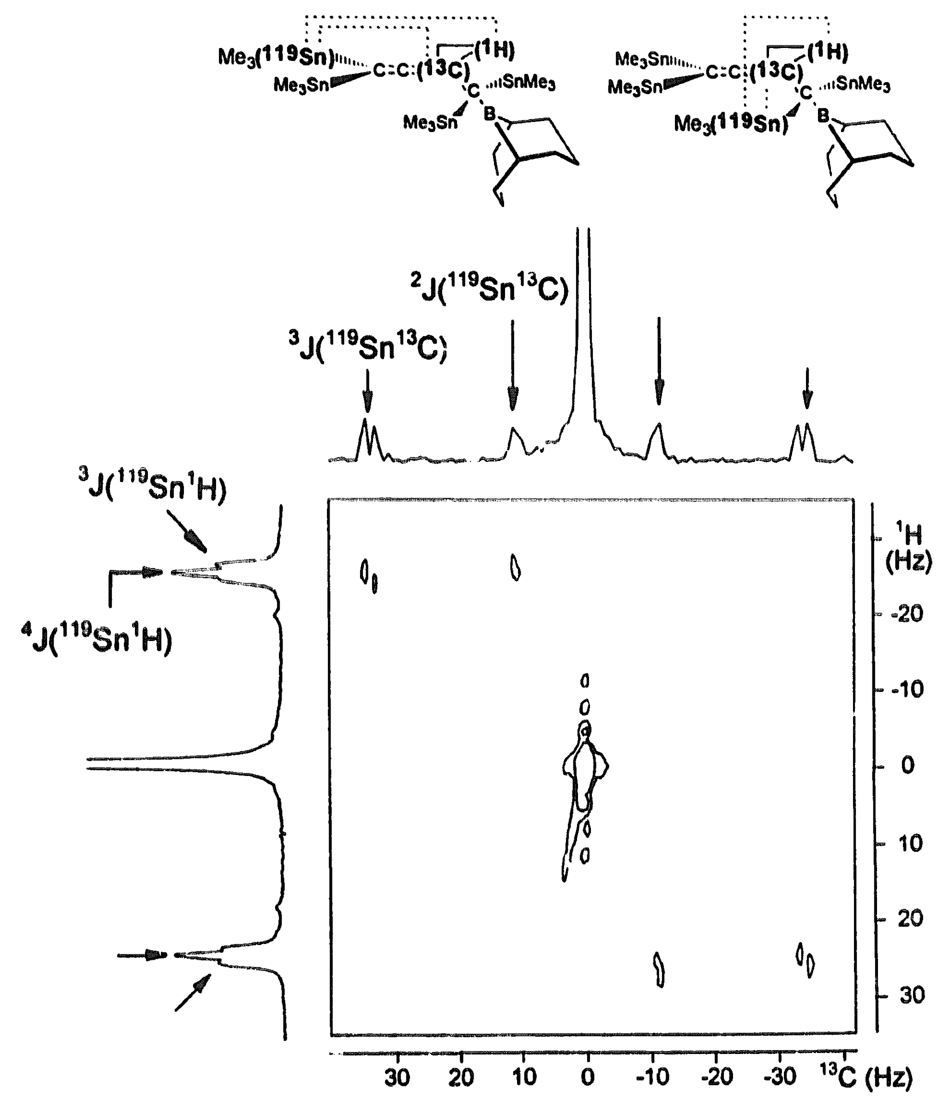

Fig. 6. Contour plot of the 125.7 MHz 2D ${}^{13}C/{}^1H$ HETCOR experiment based on ${}^1J(={}^{13}C, {}^1H)$ showing the region of the ${}^{13}C(=C-H)$ and ${}^1H(=C-H)$ resonances with the ${}^{117/119}Sn$ satellites. The full line in each formula shows the path of polarization transfer (active spins ${}^{13}C$ and ${}^1H$), and the dashed lines show the coupling constants for which the signs can be compared. The tilt of the cross peaks for the respective satellites indicates the relative sign.

3. Conclusions

As has been suggested previously, the reaction of the organometallic-substituted alkenes of type **5** or **6** with 1-alkynyltin compounds such as **4** provides a convenient way to stannyl substituted allenes. The molecular structures of **1** and **2** indicate Sn–C hyperconjugation, which is also evident from coupling constants $^1J(^{119}Sn, ^{13}C)$ and chemical shifts $\delta^{11}B$. The signs of $^nJ(^{119}Sn, ^1H)$, $^nJ(^{119}Sn, ^{13}C)$ and $^nJ(Sn,Sn)$ have been determined using 2D HETCOR experiments. The signs of the coupling constants involving the ^{119}Sn nucleus correspond to those found for $^nJ(^1H, ^1H)$ $(n = 2, 4, 5)$ in organo-substituted allenes.

4. Experimental

All preparative work was carried out in an atmosphere of dry N_2 or Ar, observing all precautions to exclude oxygen or traces of moisture. The starting materials were prepared following literature procedures. bis(trimethylstannyl)ethyne (**4**) [21], triethylborane [22], ferrocenyl–dimethylborane [23] and $(9\text{-BBN})_2$ [24]. The allenes **1** and **3** were prepared and isolated in essentially quantitative yield as described [3–5], and the same procedure was used successfully for the synthesis of **2**. The intermediate **6** was prepared by the 1 : 1 reaction of **4** with ferrocenyl–dimethylborane on a small scale for

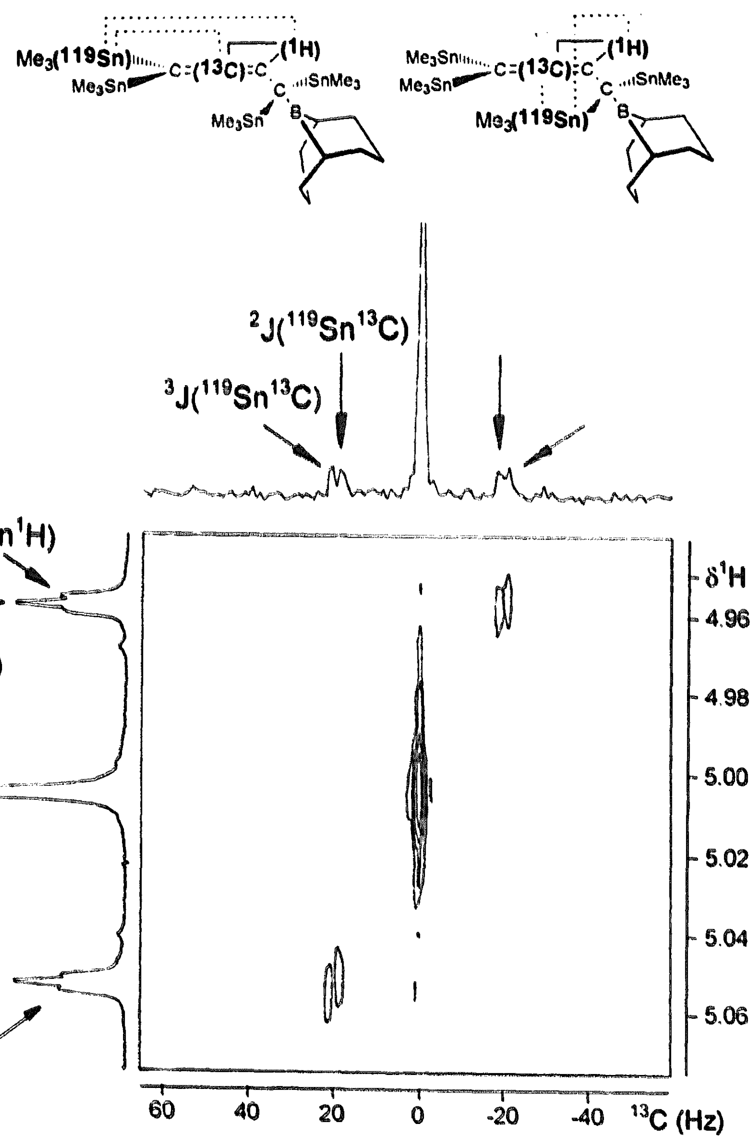

Fig. 7. Contour plot of the 125.7 MHz 2D $^{13}C/^1H$ HETCOR experiment based on $^2J(=^{13}C=C^1H)$ showing the region of the $^{13}C(=C=)$ and $^1H(=C-H)$ resonances with the $^{117/119}Sn$ satellites. The full line in each formula shows the path of polarization transfer (active spins ^{13}C and ^1H), and the dashed lines show the coupling constants for which the signs can be compared. The tilt of the cross peaks for the respective satellites indicates the relative sign.

NMR measurements (see Table 2). The allene **1** was recrystallized several times from hexane solutions until suitable single crystals (m.p. 68–70°C) could be obtained. Compound **3** gave single crystals (m.p. 112.5°C) by slow evaporation of a concentrated benzene solution. In the case of the allene **2**, all attempts at its crystallization gave a red microcrystalline material [m.p. > 110°C (decomp.)].

4-(Ferrocenyl-methylboryl)-3-methyl-1,1,4,4-tetrakis(trimethylstannyl)-1,2-butadiene (**2**): ^{1}H NMR (C_6D_6): δ^1H [$J(^{119}$Sn, ^{1}H)] = 0.16 [51.6] s, 18H, $(Me_3Sn)_2$(B)C; 0.18 [52.4] s, 18H, $(Me_3Sn)_2$C=; 0.81 [5.2] s, 3H, MeB; 1.74 [29.5] s, 3H, MeC=; 3.91 s, 5H, Cp; 4.22 m, 2H, H(2,5); 4.37 m, 2H, H(3,4).

NMR spectra in solution were recorded by using Bruker ARX 250, Bruker AC 300 or Bruker AM 500 spectrometers, all equipped with multinuclear units (see also Tables 2 and 3). Chemical shifts are given with respect to Me_4Si [δ^1H(C_6D_5H) = 7.15; δ^{13}C(C_6D_6) = 128.0], Et_2O–BF_3 [δ^{11}B = 0; $\Xi(^{11}$B) = 32.083971 MHz], and Me_4Sn [δ^{119}Sn = 0; $\Xi(^{119}$Sn) = 37.290665 MHz]. Coupling constants are accurate to ±0.5 Hz for all measurements at room temperature, and ±1 Hz for measurements at low temperature. The pulse lengths and delays for the HETCOR experiments were optimized by corresponding 1D refocused INEPT experiments with ^{1}H decoupling [25]. The solid-state ^{119}Sn CP/MAS NMR spectrum of **1** (see Fig. 4) was mea-

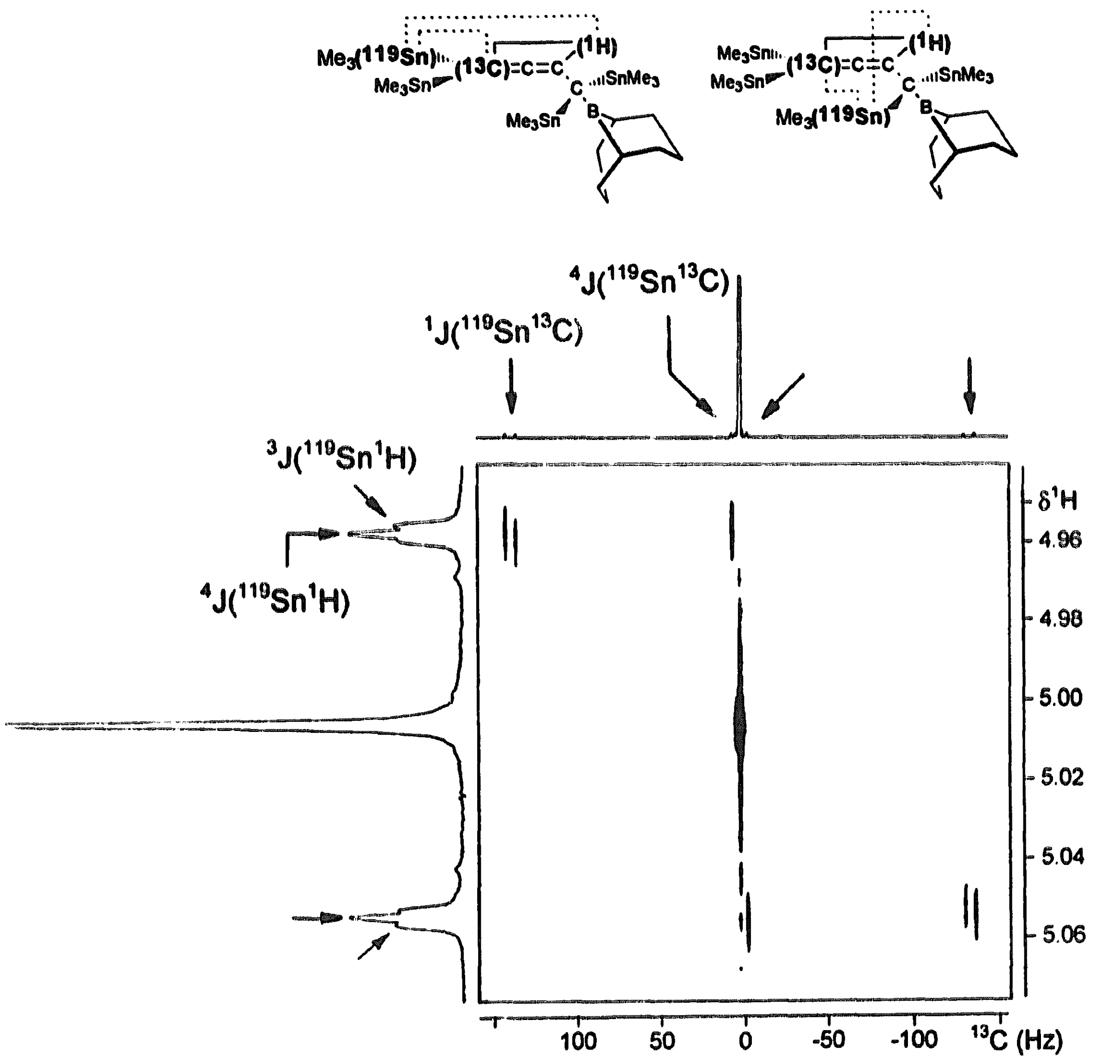

Fig. 8. Contour plot of the 125.7 MHz 2D ^{13}C/^{1}H HETCOR experiment based on $^3J(^{13}$C=C=C^{1}H) showing the region of the ^{13}C(C=) and ^{1}H(=C–H) resonances with the $^{117/119}$Sn satellites. The full line in each formula shows the path of polarization transfer (active spins ^{13}C and ^{1}H), and the dashed lines show the coupling constants for which the signs can be compared. The tilt of the cross peaks for the respective satellites indicates the relative sign.

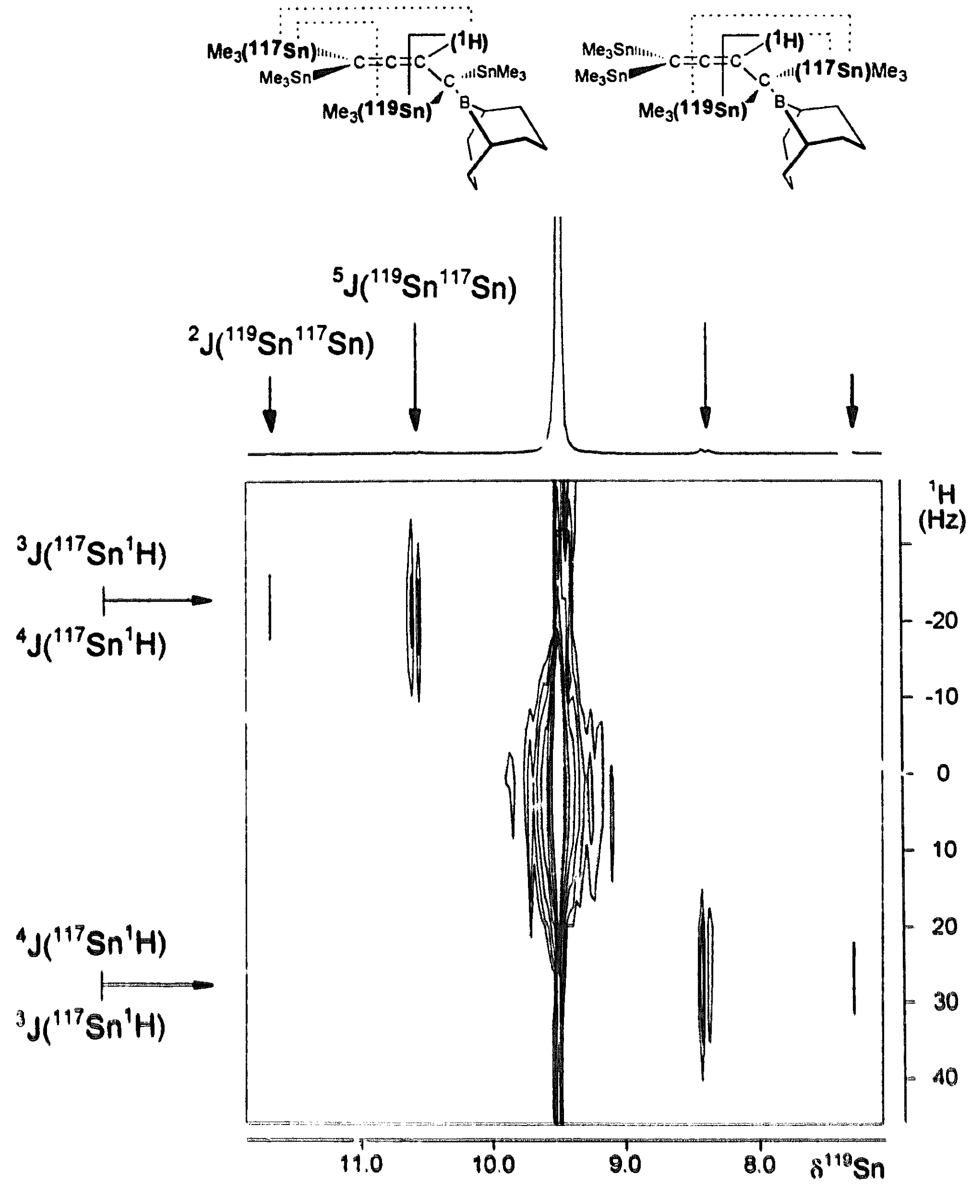

Fig. 9. Contour plot of the 111.9 MHz 2D ^{119}Sn/^{1}H HETCOR experiment based on $^{3}J(^{119}SnCC^{1}H)$ showing the region of the $^{119}Sn(Sn_2(B)C)$ NMR signal with the $^{117/119}$Sn satellites. The full line in each formula shows the path of polarization transfer (active spins ^{119}Sn and ^{1}H), and the dashed lines show the coupling constants (^{117}Sn is the passive nucleus) for which the signs can be compared. The tilt of the cross peaks for the respective satellites indicates the relative sign.

sured on a Bruker MSL 300 instrument. The air- and moisture-sensitive compound 1 was packed into an air-tight insert which fitted exactly into the commercial ZrO_2 rotor [26]. Tetracyclohexyltin served as secondary external reference for δ^{119}Sn [27].

Acknowledgements

Support of this work by the Volkswagen Stiftung, the Deutsche Forschungsgemeinschaft, and the Fonds der Chemischen Industrie is gratefully acknowledged. We thank Dr. A. Sebald for recording the solid-state ^{119}Sn CP/MAS NMR spectrum of compound 1.

References and notes

[1] (a) M. Pereyre, J.-P. Quintard and A. Rahm, *Tin in Organic Synthesis*, Butterworth, London, 1987. (b) I. Omae, *Organotin Chemistry*, J. Organomet. Chem. Library Vol. 21, Elsevier, Amsterdam, 1989.
[2] B. Wrackmeyer, *Coord. Chem. Rev.*, *145* (1995) 125.
[3] B. Wrackmeyer, *Z. Naturforsch., Teil B*, *33* (1978) 385.

[4] (a) B. Wrackmeyer and R. Zentgraf, *J. Chem. Soc., Chem. Commun.*, (1978) 402. (b) B. Wrackmeyer, *J. Organomet. Chem.*, *205* (1981) 1.

[5] (a) B. Wrackmeyer and C. Bihlmayer, *J. Chem. Soc., Chem. Commun.*, (1981) 1093. (b) B. Wrackmeyer, C. Bihlmayer and M. Schilling, *Chem. Ber.*, *116* (1983) 3182.

[6] (a) A. Berndt, *Angew. Chem.*, *105* (1993) 1034; *Angew. Chem., Int. Ed. Engl.*, *32* (1993) 985. (b) C. Wieczorek, J. Allwohn, G. Schmidt-Lukasch, R. Hunold, W. Massa and A. Berndt, *Angew. Chem.*, *102* (1990) 435; *Angew. Chem., Int. Ed. Engl.*, *29* (1990) 398.

[7] (a) G. Menz and B. Wrackmeyer, *Z. Naturforsch., Teil B*, *32* (1977) 1400. (b) B. Wrackmeyer, *Polyhedron*, *5* (1986) 1709.

[8] B. Wrackmeyer, U. Dörfler, W. Milius and M. Herberhold, *Z. Naturforsch., Teil B*, *51* (1996) 851.

[9] Further details of the crystal structure analyses are available on request from the Fachinformationszentrum Karlsruhe, Gesellschaft für wisseschaftlich-technische Information mbH, D-76344 Eggenstein-Leopoldshafen, Germany on quoting the depository numbers CSD-405141 (**1**) and CSD-405142 (**3**), the names of the authors and the journal citation.

[10] (a) G.A. Olah, G.K.S. Prakash, J.G. Shih, V.V. Krishnamurthy, G.D. Mateescu, G. Liang, G. Sipos, V. Buss, T.M. Gund, P.v.R. Schleyer, *J. Am. Chem. Soc.*, *107* (1985) 2764. (b) T. Laube, *Angew. Chem.*, *98* (1986) 368; *Angew. Chem., Int. Ed. Engl.*, *25* (1986) 349.

[11] T. Laube, *Acc. Chem. Res.*, *28* (1995) 399.

[12] A. Abragam, *The Principles of Nuclear Magnetism*, Oxford University Press, Oxford, 1961, pp. 309–312.

[13] W.S. Brey, in W.S. Brey (ed.), *Pulse Methods in 1D and 2D Liquid-Phase NMR*, Academic Press, New York, 1988, pp. 1–109.

[14] J.E. McMurry, T. Lectka and C.N. Hodge, *J. Am. Chem. Soc.*, *111* (1989) 8867 and references cited therein.

[15] H. Nöth and B. Wrackmeyer, Nuclear magnetic resonance spectroscopy of boron compounds, in P. Diehl, E. Fluck and R. Kosfeld (eds.), *NMR – Basic Principles and Progress*, Vol. 14, Springer, Berlin, 1978.

[16] A. Bax and R. Freeman, *J. Magn. Reson.*, *45* (1981) 177.

[17] (a) W. McFarlane, *J. Chem. Soc. A*, (1967) 528. (b) J.D. Kennedy and W. McFarlane, *J. Chem. Soc., Chem. Commun.*, (1974) 983.

[18] B. Wrackmeyer and G. Kehr, *Z. Naturforsch., Teil B*, *49* (1994) 1407.

[19] B. Wrackmeyer, G. Kehr and J. Süß, *Main Group Met. Chem.*, *18* (1995) 127.

[20] B. Wrackmeyer, *J. Magn. Reson.*, *59* (1984) 141.

[21] (a) W.E. Davidsohn and M.C. Henry, *Chem. Rev.*, *67* (1967) 73. (b) B. Wrackmeyer, in R.B. King and J.J. Eisch (eds.), *Organometallic Syntheses*, Vol. 4, Elsevier, New York, 1988, p. 559.

[22] R. Köster, P. Binger and W.V. Dahlhoff, *Synth. React. Inorg. Metal-org. Chem.*, *3* (1973) 359.

[23] T. Renk, W. Ruf and W. Siebert, *J. Organomet. Chem.*, *120* (1976) 1.

[24] E.F. Knights and H.C. Brown, *J. Am. Chem. Soc.*, *90* (1968) 5280.

[25] (a) D.P. Burum and R.R. Ernst, *J. Magn. Reson.*, *39* (1980) 163. (b) G.A. Morris, *J. Magn. Reson.*, *41* (1980) 185.

[26] L.H. Merwin, A. Sebald, J.E. Espidel and R.K. Harris, *J. Magn. Reson.*, *84* (1989) 367.

[27] R.K. Harris and A. Sebald, *Magn. Reson. Chem.*, *25* (1987) 1058.